Voltage-tuned resonant reflectance optical filter for visible wavelengths fabricated by nanoreplica molding

Fuchyi Yang, Gary Yen, and Brian T. Cunningham[a)]
Nano Sensors Group, Department of Electrical and Computer Engineering, University of Illinois at Urbana-Champaign, 208 N. Wright Street, Urbana, Illinois 61801 and Micro and Nanotechnology Laboratory, University of Illinois at Urbana-Champaign, 208 N. Wright Street, Urbana, Illinois 61801

(Received 19 April 2007; accepted 3 June 2007; published online 26 June 2007)

A guided-mode resonant filter incorporating an electro-optically tunable liquid crystal refractive index is demonstrated at a wavelength of 655 nm and a tuning range of 4 nm. Rigorous coupled wave analysis and finite difference time domain analysis are used to simulate the characteristics of the filter during liquid crystal reorientation. Tuning performance is demonstrated that is consistent with the device simulations. Tunable filters in the visible wavelength range that are inexpensively fabricated over large surface areas are expected to find applications in optical limiting and video display. © *2007 American Institute of Physics*. [DOI: 10.1063/1.2752128]

The ability to selectively reflect specific wavelength bands and to easily tune the reflected wavelength is of interest to a broad range of optical systems, including wavelength division multiplexing,[1] spectroscopy,[2] fluorescence microscopy,[3] optical limiting for protection of sensors/eyes,[4] and video display.[5] Ideally, such a system would be capable of rapid tuning over a large wavelength range with relatively small voltages and currents, using a device that is simple and inexpensive to fabricate. Depending on the application, the reflected wavelength range may be required to be extremely narrow or broad, but the tuning range must be large enough to allow substantial modulation of reflected or transmitted intensity.

Reflectance filters based on anomalous optical resonances[6–10] that occur within certain periodic surface structures represent a class of devices that can provide 100% reflection efficiency at the resonant wavelength over a wavelength range that can be selected to be either extremely narrow (<0.5 nm) or broad (>20 nm).[10–13] Such devices, often called guided-mode resonance filters (GMRF) or surface photonic crystals (PC), are especially attractive as filters because they require the deposition of only one dielectric thin film and can be designed for wavelengths ranging from ultraviolet[14] to infrared.[10,13,15] However, the period of the structure must be substantially less than the free-space wavelength of the filtered light, providing a challenge to inexpensive fabrication approaches, particularly for producing large device areas and visible wavelength applications. Recently, plastic-based replica molding approaches have been applied to produce surface PC filters[16] that enable production upon flexible sheets of plastic film in continuous rolls for application as optical biosensors.[17–19] For many years, the ability to tune the resonant wavelength of such devices by variation of the refractive index of one of the device components has been recognized,[20] although dynamic tuning has only been demonstrated in few cases.[15,21–23]

In this work, we present the design, simulation, fabrication, and characterization of a linear grating resonance reflectance filter that incorporates integrated transparent electrodes to actuate a change in the anisotropic refractive index with a liquid crystal (LC) film. Rigorous coupled wave analysis (RCWA) and finite difference time domain (FDTD) analysis are used to simulate the device structure and to design the structural and optical parameters to obtain resonant optical modes in the visible wavelength range with narrow or broad resonances, depending on the incident light polarization with respect to the grating lines. A replica molding method is used to fabricate the subwavelength periodic surface structure, and the device is characterized by measurement of the resonant wavelength as a function of applied voltage across the LC film.

A schematic cross-sectional diagram of the device is shown in Fig. 1. The periodic surface structure is produced within a UV-cured polymer (UVCP) material as described below upon a glass substrate with an indium tin oxide (ITO) transparent conductor thin film on its surface. A high refractive index thin film of titanium dioxide (TiO_2) is deposited over the surface structure, and a thin layer of LC is distributed between the grating structure and an upper ITO-coated glass slide. An electric field is applied across the LC film by application of a dc voltage between the lower and upper ITO electrodes. In this letter, the z axis refers to the direction perpendicular to the device surface, the x axis refers to the

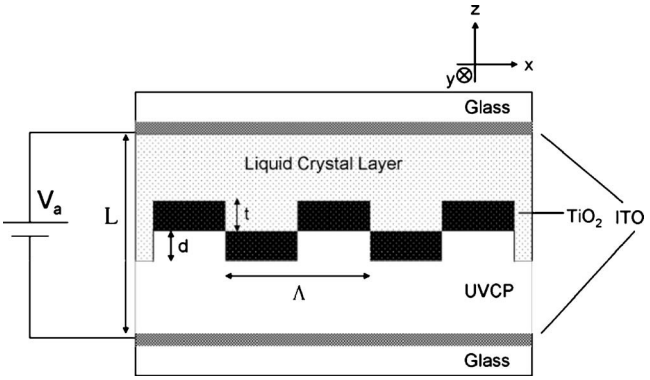

FIG. 1. Cross-sectional schematic view of the fabricated device is shown. The linear grating period is $\Lambda=360$ nm with a grating height of $d=70$ nm. The thickness of the TiO_2 layer is $t=130$ nm, and the distance between the electrodes is $L=25$ μm. Voltage is applied perpendicular to the device and across the LC layer.

a)Author to whom correspondence should be addressed; electronic mail: bcunning@uiuc.edu

 © 2007 American Institute of Physics
Downloaded 08 Jan 2010 to 128.174.191.27. Redistribution subject to AIP license or copyright; see http://apl.aip.org/apl/copyright.jsp

direction perpendicular to the grating lines, and the y axis is parallel to the grating lines as shown. Light is incident upon the structure from the bottom, propagating in the $+z$ direction with its electric field oriented either perpendicular to the grating lines (TM mode) or parallel to the grating lines (TE mode). At the resonant wavelength for TM illumination, an optical standing wave develops that is evanescently coupled to the structure surface that has an electric field vector oriented in the z direction. Likewise, at the resonant wavelength for TE illumination, an optical standing wave develops with its electric field oriented in the y direction. The peak wavelengths of resonant reflection are referred to as the peak wavelength value (PWV) and are measured separately for the TE and TM modes. With zero voltage applied between the electrodes, the LC molecules assume a random orientation. However, when a voltage is applied, the LC molecules reorient with their long axis along the z direction, resulting in an increased refractive index in the z direction but simultaneously a decreased refractive index in the x and y directions. Therefore, with applied voltage, the PWV for TM modes will increase, while the PWV for TE modes will decrease.

The resonance filter was fabricated with a nanoreplica molding process using a silicon "master" wafer as a mold template to produce a "daughter" tool from poly-dimethylsiloxane (PDMS) (Sylgard 184, Dow Chemical). The PDMS tool, in turn, is used to mold the resonance filter surface structure. The silicon master is an 8 inch diameter wafer upon which a linear grating structure with a period of 360 nm and an ~50% duty cycle is patterned by deep-UV photolithography. The grating pattern is etched into the silicon wafer to a depth of 70 nm by reactive ion etching. To produce PDMS daughter molds, the mixture (1:10 ratio of curing agent to base) was poured on top of the master and allowed to spread to a uniform thickness. PDMS was cured at 90 °C for 24 h and then released from the master to create a negative image of the silicon wafer grating structure.

An ITO-coated glass slide (Sigma-Aldrich) was used as the device substrate. A drop of UVCP, PP1-ZPUA (Gelest), was placed on the glass slide and the PDMS stamp was laid down over the top of the UVCP, allowing it to spread throughout the surface features of the PDMS stamp. With the stamp still impressed, the UVCP was cured with a UV lamp for 90 s. The stamp was then released, leaving a cured UVCP layer with features of 180 nm lines. Subsequently, TiO_2, serving as the high index layer, was deposited on top of this UVCP layer by sputter deposition.

The nematic liquid crystal 4′-pentyl-4-biphenylcarbonitrile (5CB) (Sigma) served as the electro optic material in the device. 5 μl of 5CB was pipetted on top of the TiO_2 layer. Another ITO coated glass slide was used as the upper electrode, so the two glass substrates sandwiched the liquid crystal layer. A 25 μm thick, double sided adhesive was used as a spacer to hold the two glass slides together and to determine the spacing between the upper and lower substrates. Wires were connected to the ITO films using conductive epoxy which facilitated the application of voltage.

The reflection spectrum of the device was observed using the following setup. A broadband tungsten-halogen lamp (Ocean Optics) connected to one end of a bifurcated fiber optic cable was used as the incident light source. The light travels through a linear polarizer before it illuminates the device through the bottom glass substrate. The linear polarizer can be rotated with respect to the filter grating lines so that either TE or TM illumination can be applied. The device sits flat on a stage holder and is oriented such that the light passes through the UVCP layer before the liquid crystal layer. The reflected light returns through the same linear polarizer and back into an optical fiber connected to a spectrometer (Ocean Optics). This setup is able to observe the PWV as a function of applied voltage.

RCWA (RSoft) and FDTD (Lumerical) simulations were used to explore the behavior of the filter with a liquid crystal superstrate. The filter is illuminated from below with a plane-wave source at normal incidence. The reflection spectrum had a spectral resolution of 0.1 nm and range of 650–750 nm. Simulations of the filter show a TM peak located at 655 nm and a TE peak located at 700 nm, and a reflection efficiency of 100% is predicted for both peaks. The TM resonance has a much narrower full width at half maximum (FWHM) of 0.5 nm than the TE resonance with FWHM of 49 nm. These simulations were performed with the refractive index of the LC set to $n=1.62$, corresponding to the expected value of the liquid crystal refractive index under no applied voltage.

FDTD simulations were performed to ascertain the response of the filter with variable refractive index anisotropy. With FDTD, it is possible to define a tensor for the refractive index and thus independently change the individual refractive indices in three principal directions. The device is illuminated with a plane wave at normal incidence traveling in the $+z$ direction. To measure the reflection spectrum of the filter, a frequency power monitor is placed below the incident plane wave. Only plane waves that are the same polarization as the source are monitored.

Since no alignment procedure was used in preparing our liquid crystal cell, the director has no long range uniformity. Instead, it is essentially random in different regions of the cell. Thus, an average refractive index, $n=1.62$, between the extraordinary and ordinary refractive indices is experienced by incident light in the absence of applied voltage.[24] When there is an applied voltage between the two electrodes, the liquid crystal molecules will orient themselves with the long axis parallel to the electric field lines since 5CB has positive $\Delta\epsilon$. This reorientation will produce an increase in the refractive index in the z direction and simultaneously reduce the refractive indices in both the x and y directions. The FDTD simulation results validate that such behavior of the liquid crystals will result in a positive shift of the TM PWV, while producing a simultaneous negative shift of the TE PWV. The maximum possible difference between n_z and n_y is the birefringence of the liquid crystal. 5CB has a birefringence of about $\Delta n=0.20$ in the relevant wavelength range. Therefore, a maximum shift of +8.9 nm is possible for TM polarization and −5.5 nm for TE polarization, based on the initial condition of the system.

Experimental data are obtained for both polarizations using the reflection setup described earlier, but only reflection spectra for the TM polarization is shown in Fig. 2. The TM FWHM is 2.3 nm and indeed much narrower than the TE FWHM of 20.14 nm. The locations of the PWV with no applied voltage agree roughly to the values obtained with simulations. The slight differences in PWV are due to process deviations in the grating duty cycle from the intermediate PDMS molding process. Reflection spectra were taken at

Downloaded 08 Jan 2010 to 128.174.191.27. Redistribution subject to AIP license or copyright; see http://apl.aip.org/apl/copyright.jsp

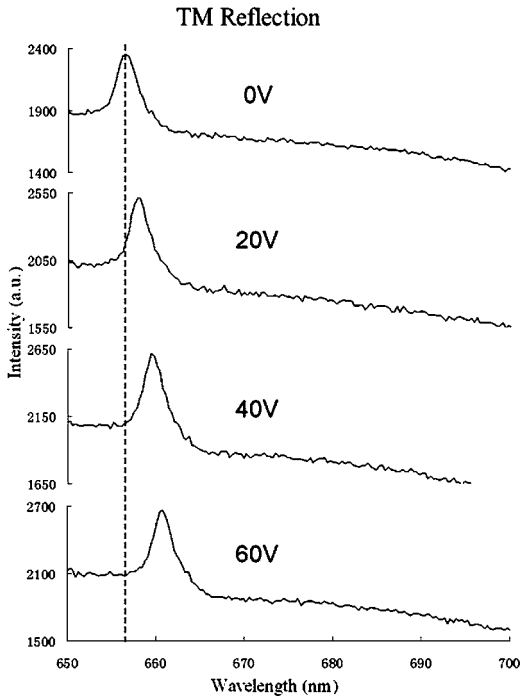

FIG. 2. TM reflection spectra at different applied voltages. The PWV shift is +4 nm at 60 V. The vertical dashed line is inserted as a visual guide to distinguish the shifted peak location.

10 V increments from 0 to 60 V. For a spacer distance of 25 μm, the maximum electric field applied to the device was 2.4 V/μm. The polarity of the applied voltage did not affect the tuning behavior of the device. However, for consistency, the cathode was applied to the top electrode and the anode was applied to the bottom electrode. At 60 V, the TM PWV shifts by +4 nm while the TE PWV by −2.5 nm. The TM PWV shift is larger than its FWHM, so effective modulation is possible using this device. All data points are plotted in Fig. 3. The PWV shift is linear with applied voltage for both TE and TM polarizations. This behavior agrees with the FDTD simulations and confirms the fact that the liquid crystal molecules are reorienting due to the presence of an electric field. Note that the TM PWV shift is greater than the TE PWV shift for the same change in refractive index. This is consistent with RCWA simulations indicating that the TM polarization has higher bulk shift sensitivity than TE polarization. Another note of interest is that the PWV shift did not level off. Thus, the maximum tuning range has not been reached yet for the current device. Decreasing the spacing between the ITO electrodes will allow larger electric field to be applied, and therefore allow the maximum shift to be achieved.

Even though the device is a reflection filter, the efficiency of the filter response is determined using a transmission setup due to feasibility. In this setup, the device has a transmission dip at the PWV. The device's transmission spectrum is normalized by a transmission spectrum with no device present. The TE PWV transmission is under 10%, while that of the TM case is only ~90%. Absorption of the LC material at the resonant wavelength is predicted to reduce the efficiency in this manner.

A guided-mode resonant filter designed to incorporate a liquid crystal with a voltage-controlled refractive index anisotropy is demonstrated for visible wavelengths. RCWA and

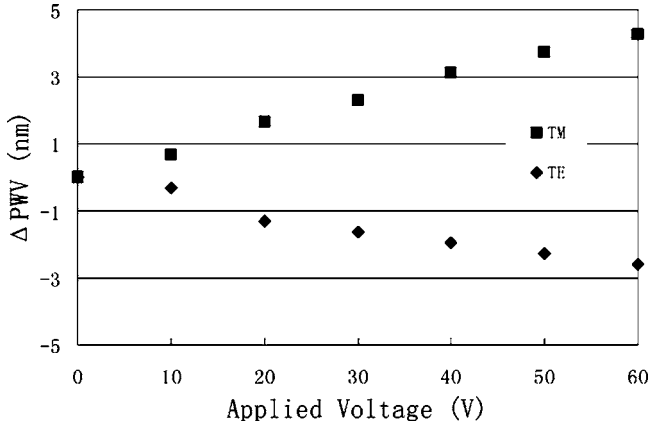

FIG. 3. Experimental data of the PWV shift as a function of applied voltage. Both TE and TM polarizations are shown.

FDTD were used to predict the resonant wavelengths, FWHM, and wavelength shift of TE and TM resonant modes. Devices were fabricated by a room temperature replica molding process to create the $\Lambda = 360$ nm period surface structure of the filter, and transparent indium tin oxide electrodes were incorporated above and below the filter to apply an electric field perpendicular to the device surface. The operating characteristics of the TE and TM resonant modes were consistent with those predicted by simulation.

This research was supported by the U.S. Army Research Office under project manager Joel Carlson under Contract No. W911QY-06-C-0043, and the authors would like to acknowledge Carlson for many helpful discussions.

[1]M. W. Maeda, J. S. Patel, C. L. Lin, J. Horrobin, and R. Spicer, IEEE Photonics Technol. Lett. **2**, 820 (1990).
[2]I. Kurtz, R. Dwelle, and P. Katzka, Rev. Sci. Instrum. **58**, 1996 (1987).
[3]M. Bouhifd, M. P. Whelan, and M. Aprahamian, Proc. SPIE **5826**, 185 (2005).
[4]M. J. Grout, Opt. Mater. (Amsterdam, Neth.) **14**, 155 (2000).
[5]Z. LI, P. Desai, R. Akins, G. Ventouris, and D. Voloschenko, Proc. SPIE **4658**, 7 (2002).
[6]R. W. Wood, Philos. Mag. **4**, 396 (1902).
[7]A. Hessel and A. A. Oliner, Opt. Commun. **59**, 327 (1986).
[8]S. S. Wang, R. Magnusson, J. S. Bagby, and M. G. Moharam, J. Opt. Soc. Am. A **7**, 1470 (1990).
[9]R. Magnusson and S. S. Wang, Appl. Phys. Lett. **61**, 1022 (1992).
[10]S. S. Wang and R. Magnusson, Appl. Opt. **32**, 2606 (1993).
[11]S. Tibuleac and R. Magnusson, Opt. Lett. **26**, 584 (2001).
[12]Z. S. Liu, S. Tibuleac, D. Shin, P. P. Young, and R. Magnusson, Opt. Lett. **23**, 1556 (1998).
[13]G. Levy-Yurista and A. A. Friesem, Appl. Phys. Lett. **77**, 1596 (2000).
[14]N. Ganesh and B. T. Cunningham, Appl. Phys. Lett. **88**, 071110 (2006).
[15]A. Sharon, D. Rosenblatt, A. A. Friesem, H. G. Weber, H. Engel, and R. Steingrueber, Opt. Lett. **21**, 1564 (1996).
[16]B. Cunningham, B. Lin, J. Qiu, P. Li, J. Pepper, and B. Hugh, Sens. Actuators B **85**, 219 (2002).
[17]B. Cunningham, P. Li, B. Lin, and J. Pepper, Sens. Actuators B **81**, 316 (2002).
[18]B. Lin, J. Qiu, J. Gerstenmeie, P. Li, H. M. Pien, J. Pepper, and B. Cunningham, Biosens. Bioelectron. **17**, 827 (2002).
[19]P. Y. Li, B. Lin, J. Gerstenmaier, and B. Cunningham, Sens. Actuators B **99**, 6 (2004).
[20]R. Magnusson and S.-S. Wang, U.S. Patent No. 5,216,680 (1 June 1993).
[21]D. W. Dobbs and B. T. Cunningham, Appl. Opt. **45**, 7286 (2006).
[22]S. Y. Chou, U.S. Patent No. 6,999,156 B2 (14 February 2006).
[23]T. Katchalski, G. Levy-Yurista, A. A. Friesem, G. Martin, R. Hierle, and J. Zyss, Opt. Express **13**, 4645 (2005).
[24]S. T. Wu, C. S. Wu, M. Warenghem, and M. Ismaili, Opt. Eng. **32**, 1775 (1993).

Downloaded 08 Jan 2010 to 128.174.191.27. Redistribution subject to AIP license or copyright; see http://apl.aip.org/apl/copyright.jsp